Supporting Information

Simple and Sensitive Colorimetric Detection of Trace Amount of 2,4,6-trinitrotoluene (TNT) with QD multilayers-modified micro-channel assays

Tao Hu,[a] Wen Sang, [a] Chen Ke, [a] Hongxi Gu, [b] Zhonghua Ni, [*a] Shaoqin Liu [*b]

a) School of Mechanical Engineering, and Jiangsu Key Laboratory for Design and Manufacture of Micro–Nano Biomedical Instruments, Southeast University, Nanjing 211189, China.

b) Key Laboratory of Microsystems and Microstructures Manufacturing, Ministry of Education, Harbin Institute of Technology, Harbin 150080, China.

*Corresponding authors: nzh2003@seu.edu.cn; shaoqinliu@hit.edu.cn

Part S1 Experimental section

Synthesis of MPA-capped CaTe QDs and L-cysteine-capped CdTe QDs

CdTe NPs were prepared by reacting Cd^{2+} and H_2Te gas in the presence of stabilizers according to the Rogach-Weller method[S1] with slight modification.[S2-S3] A 0.498 g (0.59 mmol) sample of $Cd(ClO_4)_2{\cdot}6H_2O$ and 0.498g (0.14 mmol) of L-cysteine or 0.012 mL (0.14 mmol) 3-mercaptopropionic acid (MPA) was dissolved in 62 mL distilled water. The pH was then adjusted to 11.2 by adding 1 M NaOH. The solution was placed in the three-neck flask and deaerated by N_2 gas for about 30 min. H_2Te gas generated by the mixture of 0.2 g of Al_2Te_3 and 15 mL of 0.5 M H_2SO_4 in another three-neck flask was directed into the prepared solution under a N_2 atmosphere. The precursors were converted to CdTe nanocrystals by refluxing the reaction mixture at 100 °C for several hours in N_2 gas to obtain appropriate size. Figure S1 shows typical absorption and photoluminescence spectra of CdTe QDs. The green QDs shows a fluorescence maximum at 520 nm and red QDs show a fluorescence peak at 620 nm, respectively. The sharp absorbance and photoluminescence peaks indicate the relatively narrow size distribution of both QDs samples. The size of CdTe QDs could be calculated through the wavelength of the first excitonic absorption peak of the QDs. The average particle size of above-mentioned CdTe QDs was estimated to be 1.69 nm (green QDs) and 3.47 nm (red QDs) with the UV-Vis spectrum according to the empirical equations proposed by Peng and co-workers,[S4] respectively. These results are consistent with that obtained from typical TEM image of the CdTe QDs (Figure S2).

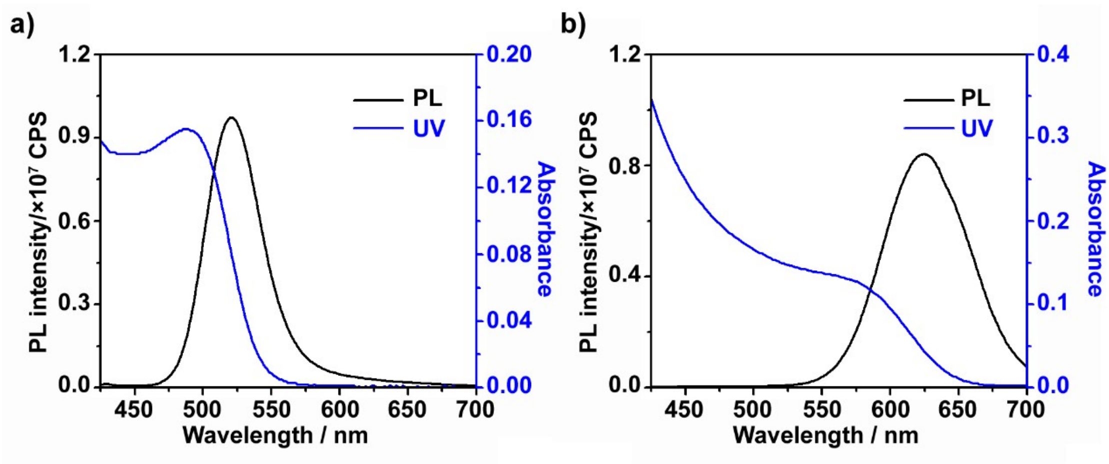

Figure S1. UV-vis absorption spectra and fluorescence spectra of green QDs(a) and red QDs(b).

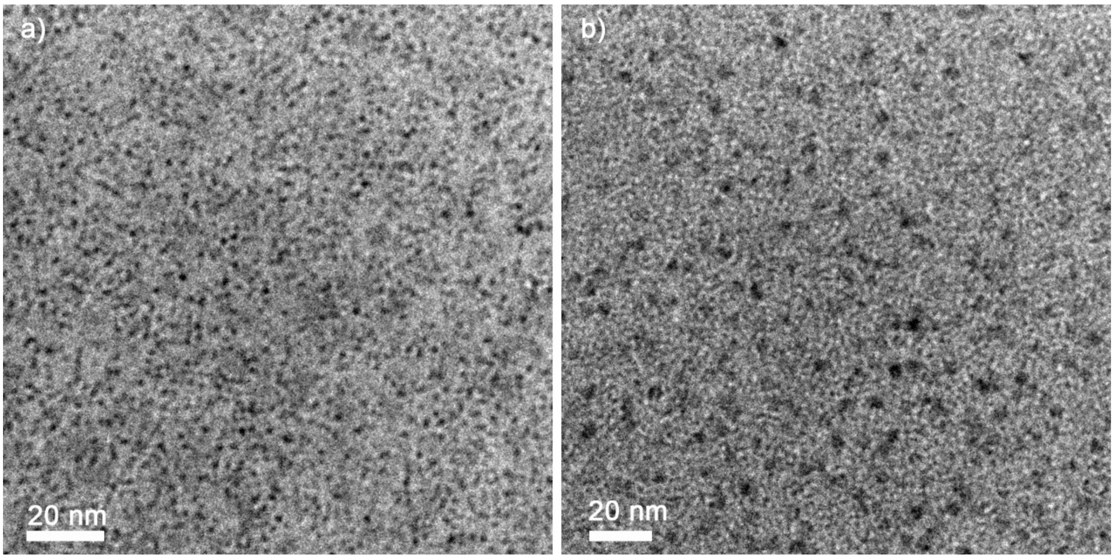

Figure S2 TEM images of green QDs and red QDs.

Fabrication of QD multilayers-coated microfluidic chips

Glass substrates and microfluidic chips were used as substrates. Glass substrates, and glass substrates of microfluidic chips was cleaned with Piranha solution (H_2O_2:H_2SO_4=3:1) at 70 ℃,[S5] followed by washed by deionized water and dried under N_2 flow.

QD multilayers-coated glass substrates were fabricated by a typical layer-by-layer (LbL) self-assembly method.[S6-S7] Firstly, the substrates were alternatively immersed into 1mg mL^{-1} positively-charged PEI solutions (pH 7.4, 1 M NaCl) and 1mg mL^{-1} negatively-charged PSS solutions (pH 7.4, 1 M NaCl) to form $(PEI/PSS)_3$ multilayers-coated glass substrates, using an immersion time of 5min, and rinsed with pure water and dried under N_2 flow after each layer deposited. Secondly, ten PAH/green QDs bilayers were alternatively deposited onto $(PEI/PSS)_3$ multilayers-coated glass substrates from 1mg mL^{-1} positively-charged PAH (pH 7.4, 1 M NaCl) and green fluorescent MPA-capped CdTe QDs solution to obtain $(PEI/PSS)_3(PAH/green\ QDs)_{10}$ multilayers. Thirdly, three bilayers of PAH/PSS were deposited onto $(PEI/PSS)_3(PAH/green\ QDs)_{10}$ multilayers from 1mg mL^{-1} positively-charged PAH solutions (pH 7.4, 1 M NaCl) and 1mg/mL negative-charged PSS solutions (pH 7.4, 1 M NaCl). Finally, five bilayers of PAH/Red QDs were deposited onto $(PEI/PSS)_3(PAH/green\ QDs)_{10}(PAH/PSS)_3$ multilayers from 1mg/mL positively-charged PAH (pH 7.4, without NaCl) and red fluorescent L-cysteine-capped CdTe QDs solution and one more PAH was deposited at the outside of the sensor film. The configuration of the multilayer was $(PEI/PSS)_3(PAH/green\ QDs)_{10}(PAH/PSS)_3$ $(PAH/red\ QDs)_5PAH$.

A PDMS microfluidic chips used in this work had a simple layout. Microfluidic channels were formed in PDMS by a photolithography technique.[S8-S9] The microfluidic chips had brief channels geometry (5 parallel lines, 50 μm wide, 30 μm deep, 3 cm long), then this chips was followed by alternate deposition of polyelectrolytes and QDs to form the hybrid film sensor in the microfluidic channels following the same procedure as QD multilayers-coated glass substrates. The micro channels were first filled with sample solution using syringe pump and allowed to incubate (no flow) for 10 min. The channels were then rinsed with water and dried. As same, the configuration of film in micro channels were also $(PEI/PSS)_3(PAH/green\ QDs)_{10}(PAH/PSS)_3(PAH/red\ QDs)_5PAH$.

Part S2 Characterization of QD multilayers-coated glass substrates and microfluidic chips

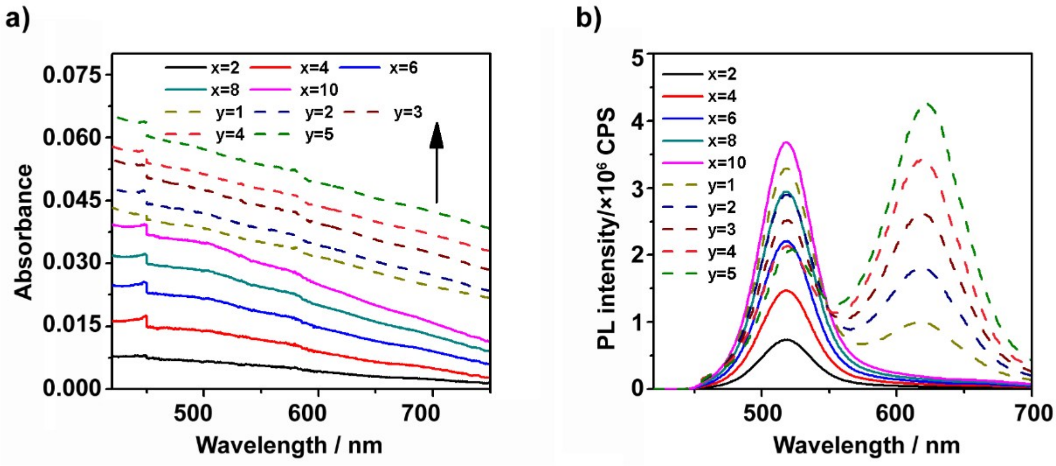

Figure S3. UV-vis (a) and fluorescent (b) spectra of QD multilayers deposited on glass substrates during LBL assembly process: $(PEI/PSS)_3(PAH/green\ QDs)_2$ (blank solid line), $(PEI/PSS)_3(PAH/green\ QDs)_4$ (red solid line), $(PEI/PSS)_6(PAH/green\ QDs)_6$ (blue solid line), $(PEI/PSS)_3(PAH/green\ QDs)_8$ (Dark Cyan solid line), $(PEI/PSS)_3$ $(PAH/green\ QDs)_{10}$ (Magenta solid line), $(PEI/PSS)_3(PAH/green\ QDs)_{10}(PAH/PSS)_3$ $(PAH/red\ QDs)_1$ (Dark Yellow Dash line), $(PEI/PSS)_3(PAH/green\ QDs)_{10}(PAH/PSS)_3$ $(PAH/red\ QDs)_2$ (Navy Dash line), $(PEI/PSS)_3(PAH/green\ QDs)_{10}(PAH/PSS)_3$ $(PAH/red\ QDs)_3$ (Wine Dash line), $(PEI/PSS)_3(PAH/green\ QDs)_{10}(PAH/PSS)_3$ $(PAH/red\ QDs)_4$ (Pink Dash line), $(PEI/PSS)_3(PAH/green\ QDs)_{10}(PAH/PSS)_3$ $(PAH/red\ QDs)_5$ (Olive Dash line).

The FRET efficiency of $(PEI/PSS)_3(PAH/green\ QDs)_{10}(PAH/PSS)_3(PAH/red\ QDs)_y$ increases with *y*, and can be calculated according to equation:[S10]

$E=1-F_{DA}/F_D$

Where F_{DA} is the 520nm QD fluorescence of $(PEI/PSS)_3(PAH/green\ QDs)_{10}(PAH/PSS)_3$ in the presence of $(PAH/red\ QDs)_y$, and F_D is the 520nm QD fluorescence of $(PEI/PSS)_3(PAH/green\ QDs)_{10}(PAH/PSS)_3$ in the absence of $(PAH/red\ QDs)_y$. The FRET efficiency of $(PEI/PSS)_3(PAH/green\ QDs)_{10}(PAH/PSS)_3(PAH/red\ QDs)_y$ is 11.7%，21.6%, 31.7%, 42.4% and 45.6% for y=1~5, respectively.

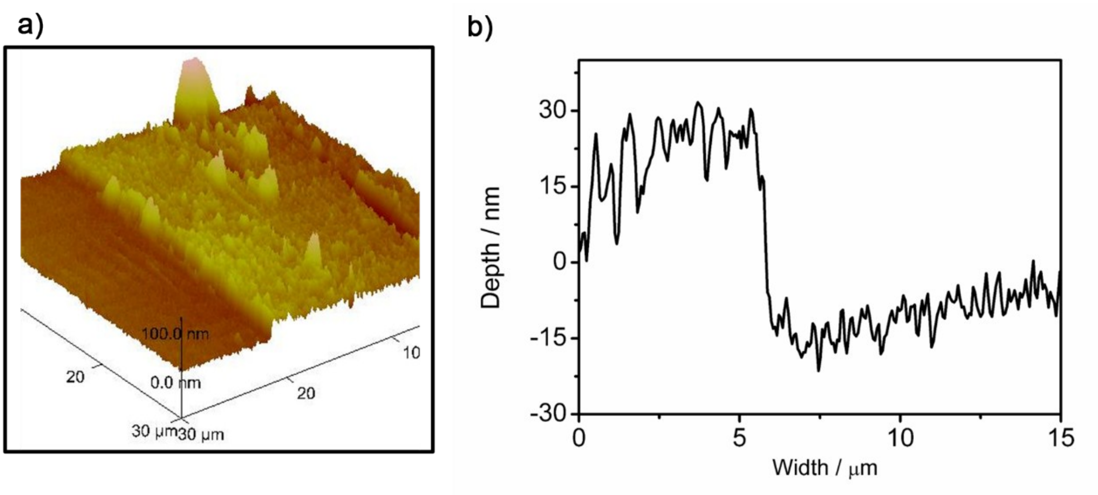

Fig. S4 AFM micrograph (tapping mode) (a) and cross-sectional analysis (b) of the QD multilayers-coated film on glass.

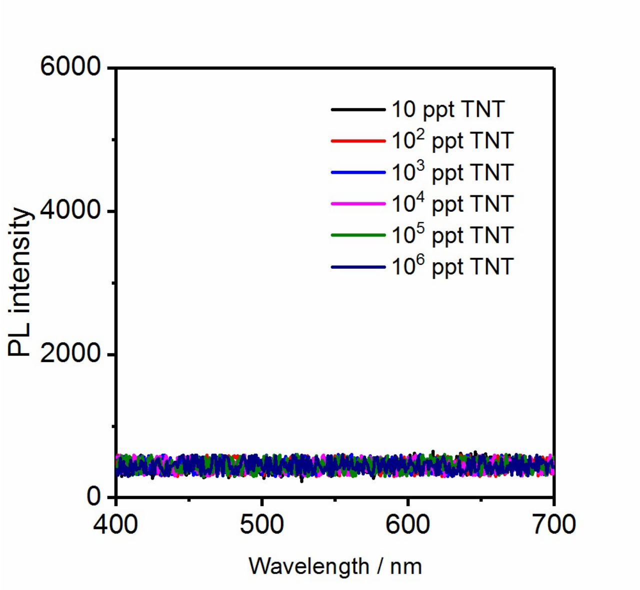

Fig. S5 FL spectra of different concentrations of TNT with 365 nm as excitation wavelength.

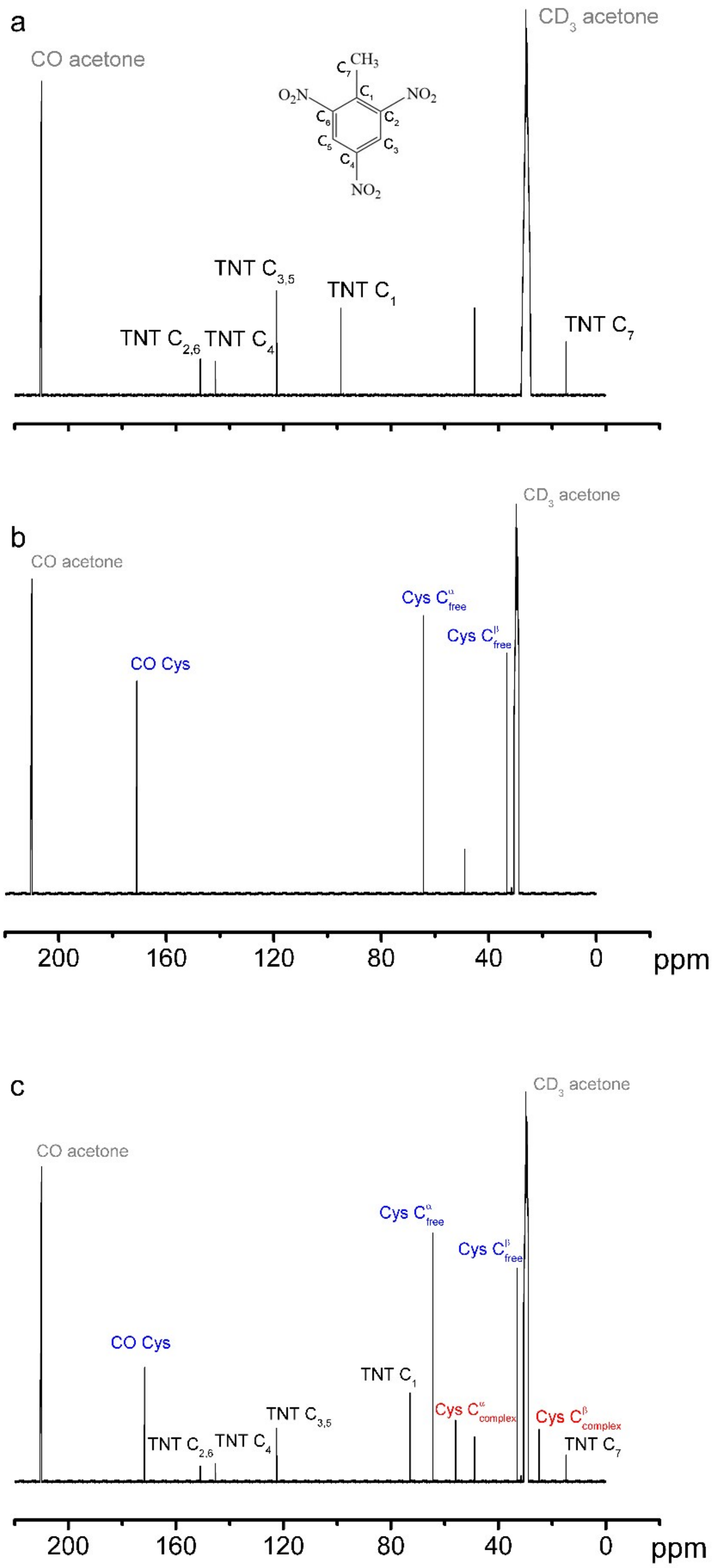

Figure S6 ^{13}C-NMR spectrum of 2,4,6-trinitrotoluene (TNT) (2 mM) (a), cysteine (6 mM) (b), and the mixture of TNT and cysteine (c) in 1/1 (by vol.) H_2O/d_6-acetone at room temperature.

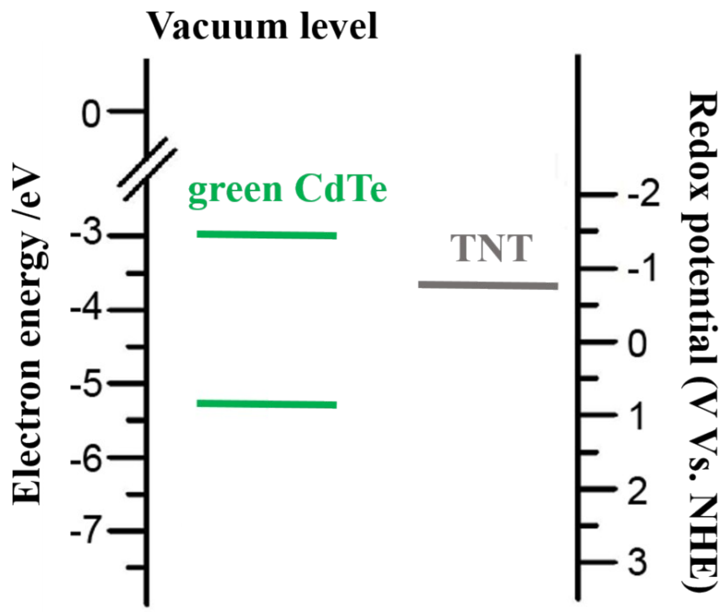

Figure S7. Energy level diagram of green CdTe QDs and the reduction potential of TNT.

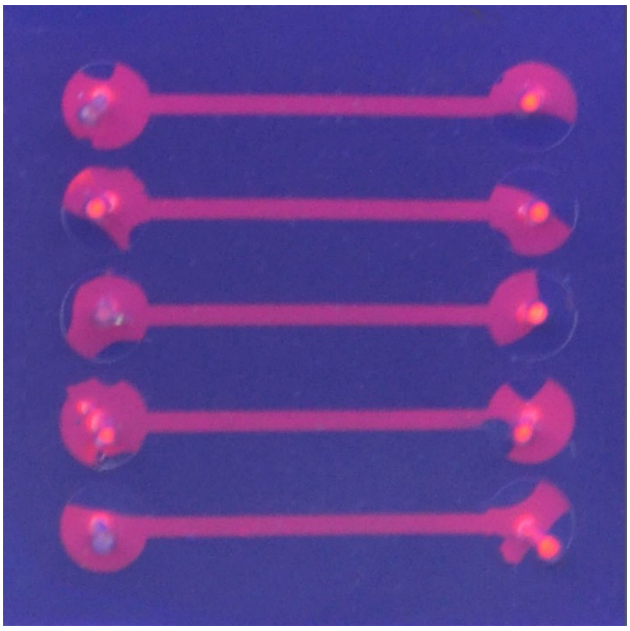

Figure S8. Photo images of QD multilayers-coated microfluidic chips.

Part S3 Performance of QD multilayers-coated microfluidic chips for TNT detection

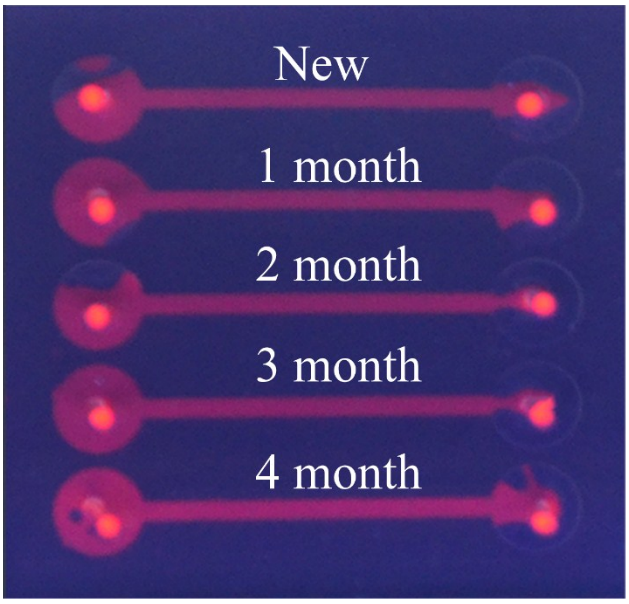

Figure S9. Stability of QD multilayers-coated microfluidic chips.

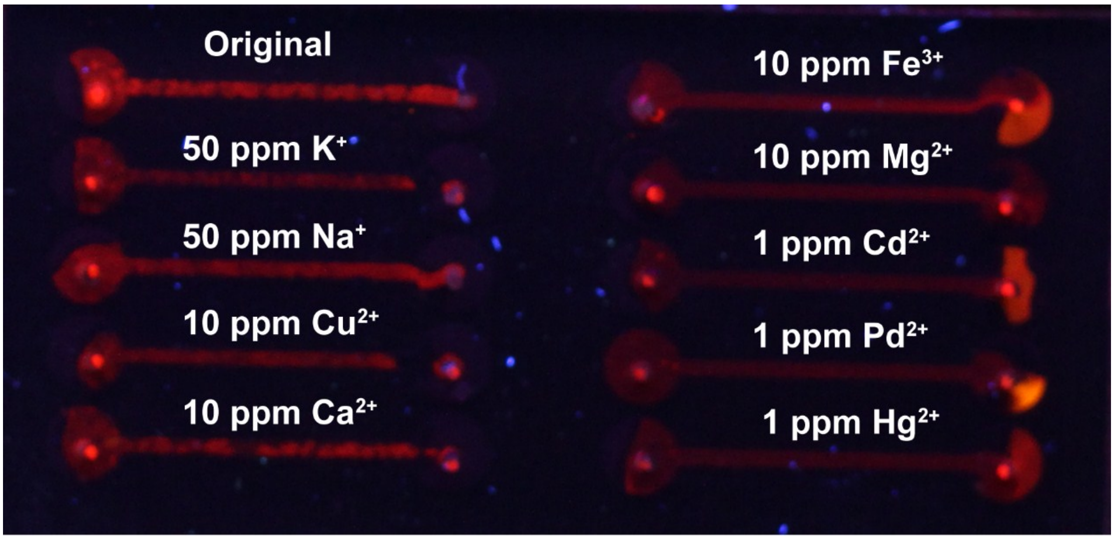

Figure S10. Response of $(PEI/PSS)_3(PAH/\text{green QDs})_{10}(PAH/PSS)_3(PAH/\text{red QDs})_5$ multilayers-based microchannel assays toward different common ions.

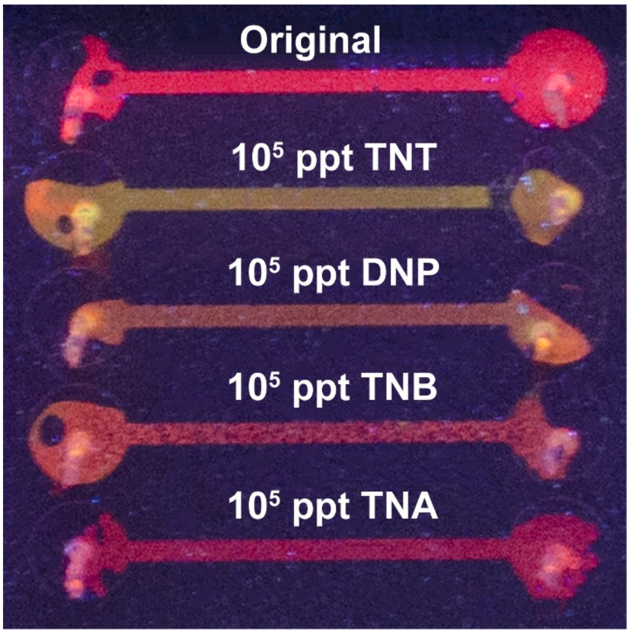

Figure S11. Response of $(PEI/PSS)_3(PAH/green\ QDs)_{10}(PAH/PSS)_3(PAH/red\ QDs)_5$ multilayers-based microchannel assays toward different TNT analogs spiked in Jiulong Lake water. The concentration of TNT analogs is 10^5 ppt.

Table S1 Comparison the proposed method and other TNT sensors.

Detection method	LOD	Linear range	Detection time	Reference
Fluorescence of MIP-capped CdSe QDs	6.16×10^4 ppt	1.76×10^5- 6.6×10^7 ppt	5 mins	S11
Fluorescence of amine-Capped ZnS-Mn^{2+} QDs	200 ppt	-	5 mins	S12
Fluorescence of creatinine-capped CdSe/ZnS QDs	3.37×10^3 ppt	10^4 - 3×10^5 ppt	5 mins	S13
Fluorescence of MoO_x QDs	2.64×10^3 ppt	1.1×10^4 - 5.3×10^5 ppt	5 mins	S14
Fluorescence of histidine-capped CdSe/ZnS QDs	4.1×10^4 ppt	4.1×10^4 -10^7 ppt	60 mins	S15
Fluorescence of L-cysteine-capped CdTe QDs	400 ppt	-	120 mins	S16
Fluorescence of L-cysteine-capped Co^{2+} dopped ZnS QDs	2.5×10^3 ppt	2.5×10^3 - 1.1×10^5 ppt	5 mins	S17
FRET between QDs/Antibody Fragment hybrid	2×10^4 ppt	9.8×10^3 - 10^7 ppt	10 mins	S18
FRET between gold nanorod-CdTe/CdS QDs	22 ppt	22 - 13.2×10^3 ppt	10 mins	S19

hybrid				
Ratiometric Fluorescence with red CdTe QDs@SiO2@green CdTe QDs	4×10^{3} ppt	4×10^{3} - 10^{4}ppt	3 mins	S20
Ratiometric Fluorescence with red Cu-ZnCdS QDs@SiO2@green ZnCdS QDs	1.1×10^{5} ppt	8.8×10^{7}- 8.8×10^{8} ppt	10 mins	S21
Ratiometric Fluorescence with green QDs@SiO2@red QDs	7.5×10^{3} ppt	2.2×10^{3} -1.7×10^{6} ppt	10 mins	S22
Ratiometric Fluorescence with QDs multilayer-modified microfluidic chip	5.24 ppt	10 - 10^{7} ppt	5 mins	This study

REFERENCES

S1 N. Gaponik, D. V. Talapin, A. L. Rogach, K. Hoppe, E. V. Shevchenko, A. Kornowski, *J. Phys. Chem. B.*, 2002, **106**, 7177-7185.

S2 Y. Zhou, Z. Zhu, W. Huang, W. Liu, S. Wu, X. Liu, Y. Gao, W. Zhang, Z. Tang, *Angew. Chem. Int. Ed.*, 2011, **50**, 11456-11459.

S3 T. Hu, B. P. Isaacoff, J. H. Bahng, C. Hao, Y. Zhou, J. Zhu, X. Li, Z. Wang, S.

Liu, C. Xu, J. S. Biteen, N. A. Kotov, *Nano Lett.*, 2014, **14**, 6799-6810.

S4 W. W. Yu, L. H. Qu, W. Z. Guo, X. G. Peng, *Chem. Mater.* 2003, **15**, 2854-2860.

S5 D. G. Kurth, T. Bein, *Langmuir*,1993, **9**, 2965-2973.

S6 G. Decher, *Science*, 1997, **277**, 1232-1237.

S7 Z. Tang, Y. Wang, P. Podsiadlo, N. A. Kotov, *Adv. Mater.*, 2006, 18, 3203-3224.

S8 D. C. Duffy, J. C. McDonald, O. J. Schueller, G. M. Whitesides, *Anal. Chem.*, 1998, 70, 4974-4984.

S9 J. C. McDonald, G. M. Whitesides, *Acc. Chem. Res.*, 2002, **35**, 491-499.

S10 A. R. Clapp, I. L. Medintz, J. M. Mauro; B. R. Fisher, M. G. Bawewndi, H. Mattoussi, *J. Am. Chem. Soc.* 2004, **126**, 301-310.

S11 S. F. Xu, H. Z. Lu, J. H. Li, X. L. Song, A. X. Wang, L. X. Chen, S. B. Han, *ACS Appl. Mater. Inter.*, 2013, **5**, 8146-8154.

S12 R. Tu, B. Liu, Z. Wang, D. Gao, F. Wang, Q. Fang, Z. Zhang, *Anal. Chem.*, 2008, **80**, 3458-3465.

S13 C. Carrillo-Carrión, B. M. Simonet, M. Valcárcel, *Anal. Chem. Acta*, 2013, **792**, 93-100.

S14 S. J. Xiao, X. J. Zhao, P. P. Hu, Z. J. Chu, C. Z. Huang, L. Zhang, *ACS Appl. Mater. Interfaces*, 2016, **8**, 8184-8191.

S15 E. R. Goldman, I. L. Medintz, A. Hayhurst, G. P. Anderson, J. M. Mauro, B. L. Iverson, G. Georgiou, H. Mattoussi, Anal. Chem. Acta, 2005, **534** (2005) 63-67.

S16 Y. Chen, Z. Chen, Y. He, H. Lin, P. Sheng, C. Liu, S. Luo, Q. Cai, *Nanotechnology*, 2010, **21**, 125502.

S17 W. S. Zou, J. Q. Qiao, X. Hu, X. Ge, H. Z. Lian, *Anal. Chem. Acta*, 2011, **708**, 134-140.

S18 E. R. Goldman, I. L. Medintz, J. L. Whitley, A. Hayhurst, A. R. Clapp, H. T. Uyeda, J. R. Deschamps, M. E. Lassman, H. Mattoussi, *J. Am. Chem. Soc.*, 2005, **127**, 6744-6751.

S19 Y. Xia, L. Song, C. Zhu, *Anal. Chem.*, 2011, **83**, 1401-1407.

S20 K. Zhang, H. Zhou, Q. Mei, S. Wang, G. Guan, R. Liu, J. Zhang, Z. Zhang, *J. Am. Chem. Soc.*, 2011, **133**, 8424-8427.

S21 P. Wu, C. Xu, X. Hou, J.-J. Xu, H.-Y. Chen, *Chem. Sci.*, 2015, **6**, 4445-4450.

S22 J. Qian, M. Hua, C. Wang, K. Wang, Q. Liu, N. Hao, K. Wang, *Anal. Chem. Acta*, 2016, **946**, 80-87.